ENCLOSURE 2

MFN 10-013

TASC-03A, A Computer Program for Transient Analysis of a Single Channel, NEDO-32084-A Revision 2, September 2002

Non-Proprietary Information

IMPORTANT NOTICE

Enclosure 2 is a non-proprietary version of the TASC-03A, A Computer Program for Transient Analysis of a Single Channel, NEDC-32084P-A Revision 2, July 2002 from Enclosure 1, which has the proprietary information removed. The proprietary information of GEH was indicated by "bars" drawn in the right-hand margin of the text of the report (as shown to the right of this paragraph). Portions of the document that have been removed are indicated by white space with a side bar in the right margin.

GE Nuclear Energy

NEDO-32084-A
Revision 2
Class I
September 2002

TASC-03A

A COMPUTER PROGRAM FOR TRANSIENT ANALYSIS OF A SINGLE CHANNEL

DISCLAIMER OF RESPONSIBILITY

UNITED STATES
NUCLEAR REGULATORY COMMISSION
WASHINGTON, D.C. 20555-0001

March 13, 2002

MFN:02-014

Mr. James F. Klapproth, Manager
Engineering & Technology
GE Nuclear Energy
175 Curtner Ave
San Jose, CA 95125

SUBJECT: REVIEW OF NEDC-32084P, "TASC-03A, A COMPUTER PROGRAM FOR TRANSIENT ANALYSIS OF A SINGLE FUEL CHANNEL" (TAC NO. MB0564)

Dear Mr. Klapproth:

By letter dated November 20, 2000, GE Nuclear Energy (GENE) provided the subject licensing topical report (TR) supporting the use of the TASC code in boiling water reactor transient analysis. The NRC staff's review concluded that there is reasonable assurance that TASC can be used in loss-of-coolant accident, anticipated operational occurrence, and anticipated transient without scram licensing calculations.

The staff finds that the subject TR is acceptable for referencing in licensing applications to the extent specified under the limitations delineated in the report and in the associated NRC safety evaluation (SE). The enclosed SE defines the basis for acceptance of the TR.

The NRC requests that GENE publish an accepted version of the revised TR NEDC-32084P within 3 months of receipt of this letter. The accepted version shall incorporate this letter and the enclosed SE between the title page and the abstract, and add a "-A" (designating accepted) following the report identification number (i.e., NEDC-32084P-A).

If the NRC's criteria or regulations change so that its conclusion in this letter that the TR is acceptable is invalidated, GENE and/or the applicant referencing the TR will be expected to revise and resubmit its respective documentation, or submit justification for the continued applicability of the TR without revision of the respective documentation.

Pursuant to 10 CFR 2.790, we have determined that the enclosed SE does not contain proprietary information. However, we will delay placing the safety evaluation in the public document room for a period of ten (10) working days from the date of this letter to provide you with the opportunity to comment on the proprietary aspects only. If you believe that any information in the enclosure is proprietary, please identify such information line by line and define the basis pursuant to the criteria of 10 CFR 2.790.

If you have any questions, please contact Joseph Donoghue, GENE Project Manager, at (301) 415-1131.

Sincerely,

Stuart A. Richards, Director
Project Directorate IV
Division of Licensing Project Management
Office of Nuclear Reactor Regulation

Project No. 710

Enclosure: Safety Evaluation

cc w/encl: See next page

cc:
Mr. George B. Stramback
Regulatory Services Project Manager
GE Nuclear Energy
175 Curtner Avenue
San Jose, CA 95125

Mr. Charles M. Vaughan, Manager
Facility Licensing
Global Nuclear Fuel
P.O. Box 780
Wilmington, NC 28402

Mr. Glen A. Watford, Manager
Nuclear Fuel Engineering
Global Nuclear Fuel
P.O. Box 780
Wilmington, NC 28402

UNITED STATES
NUCLEAR REGULATORY COMMISSION
WASHINGTON, D.C. 20555-0001

SAFETY EVALUATION BY THE OFFICE OF NUCLEAR REACTOR REGULATION

GE NUCLEAR ENERGY TOPICAL REPORT

NEDC-32084P, "TASC-03A, A COMPUTER PROGRAM FOR TRANSIENT ANALYSIS OF A SINGLE FUEL CHANNEL"

PROJECT NO. 710

1.0 INTRODUCTION

By letter dated November 20, 2000, GE Nuclear Energy (GENE) submitted a topical report supporting the use of the TASC code in boiling water reactor transient analysis (Reference 1). TASC is used in the GE methodology for anticipated operational occurrence (AOO), anticipated transient without scram (ATWS), and loss-of-coolant accident (LOCA) analyses. GE submitted the documentation for staff review in response to an industry sponsored audit of GE analytical practices which found that TASC had never been formally reviewed, but is currently in use for licensing basis analysis. TASC was examined by the staff during an audit of GESTAR Amendment 22 analysis for GE11 fuel and was found appropriate for AOO analysis (Reference 2). This examination, however, did not constitute a formal NRC review and approval of the code.

TASC is a detailed model of an isolated fuel channel. It is used to predict the time to boiling transition for LOCA analysis, the minimum critical power ratio (MCPR) for AOO analysis, and the MCPR and peak cladding temperature for ATWS analysis. TASC uses a five equation in-homogeneous, non-equilibrium model of the flow field coupled to a heat transfer model for the fuel channel heated and power volumes. It takes inlet flow and enthalpy, outlet pressure, and power as a function of time as boundary conditions. It uses a predictor-corrector method to solve the field equations and assumes incompressible flow to decouple the momentum equation from the equations of energy and mass conservation. It has constitutive relationships for subcooled, transition, and stable film boiling. It has models for counter current flow limitations and wall friction. Interfacial friction models are not needed because TASC uses a drift flux formulation to represent inter-phasic momentum exchange. TASC predicts the rewetting of fuel following boiling transition using either user input parameters or the Iloeje correlation.

TASC is a functional replacement of the SCAT code (Reference 3). SCAT was reviewed and approved by the staff for all of the applications proposed for TASC. GENE claimed that the replacement of SCAT with TASC is an administrative change. The staff does not agree entirely with this position, because TASC uses models that differ from those in SCAT. However, the staff does agree that TASC is a functional replacement of SCAT. Furthermore, TASC is applied to small parts of lengthy, complicated analyses. Given this fact and the fact that SCAT and TASC are similar, the staff review of TASC focused on its performance relative to

applicable test data. The staff also reviewed whether TASC has the necessary physical models to predict the phenomena of interest.

2.0 DISCUSSION

As previously stated, this review considered the assessment of the code and the applicability of the models to the transients of interest. Only integral assessment against prototypical fuel assemblies was presented. This is appropriate for a code such as TASC because:

1. It can only be used to model fuel assemblies.

2. The basic models in the code are well established and assessed.

3. There are very few user options to change the nature of the solution from what is assessed.

The assessment by GENE is presented in two forms: (a) the time to boiling transition is shown or, (b) the calculated values of the change in critical power ratio relative to the initial critical power ratio (ΔCPR/ICPR) are compared to the measured ΔCPR/ICPR. Data from the GE Two Loop Test Apparatus (TLTA) and Atlas facilities is presented with data from all of GE's fuel products including their latest 10x10 designs.

Several observations can be made and applied to all of the proposed TASC calculations. First, TASC does not have a model for zirconium oxidation; therefore, TASC cannot reliably predict temperatures above 1500°F. Second, TASC does not have a model for radiation heat transfer. TASC-predicted peak cladding temperatures during conditions of high void fraction can generally be considered conservative. This affect for the conditions TASC is typically applied to will be negligible. Finally, the model for critical power during counter-current flow conditions is entirely empirical. Any predictions of CPR during counter-current flow conditions cannot be considered to be reliable unless it is confirmed that the predicted conditions mimic those used to generate the model. This will not typically be a concern for the proposed applications for TASC because counter-current flow is not likely during the limiting transients of interest.

Review of Code for LOCA Applications

TASC is used to predict early boiling transition in LOCA analysis. This typically occurs within the first several seconds of the blow-down for a large break LOCA. This value is used in subsequent codes to turn off nucleate boiling heat transfer models and turn on transition boiling models. The equations and constitutive relationships in the code model the relevant physics necessary to predict this phenomena. The assessment against both TLTA and Atlas data presented in Chapter 4 of the topical report demonstrates that the equations in TASC are solved with sufficient accuracy to be used in licensing applications. The results of the assessment demonstrate that on average TASC conservatively predicts early boiling transition to within one second. This level of accuracy is acceptable because the conditions at dryout are not changing rapidly enough within one second to significantly alter the post dryout behavior. This provides reasonable assurance that TASC can be used to predict early boiling transition for LOCA analysis.

Review of TASC for AOO Applications

TASC is used to predict ΔCPR/ICPR for AOO analysis. Once again, the dynamic portions of these transients are normally of a short duration; typically less than 10 seconds. The validation presented in Chapter 4 of the topical report that compares predicted ΔCPR/ICPR to values measured in the GE Atlas test facility demonstrates that TASC can reliably predict this parameter. This means that the implementation of the GEXL correlation into TASC is correct and the field and heat transfer equations in TASC model the physics with sufficient accuracy to allow for an acceptable prediction. The GE AOO analysis procedure statistically accounts for uncertainties in these predictions. This provides reasonable assurance that TASC can be used to predict ΔCPR/ICPR for AOO analysis.

Review of TASC for ATWS Analysis

TASC is used during ATWS analysis to predict critical power and peak cladding temperature. The peak cladding temperature (PCT) and boiling transition (if it happens at all) will occur within the first few seconds following an isolation ATWS as the reactor vessel pressurizes and then rapidly depressurizes after the safety/relief valves open. The ability of TASC to predict changes in CPR has already been discussed and is applicable to ATWS analysis. Chapter 4 of the topical report presents results of comparisons of TASC-predicted PCT to both TLTA and Atlas test data. In the comparisons, TASC is shown to conservatively predict PCT. The validation presented in Chapter 4 of the topical report shows that the TASC models capture the relevant physics because there are enough data presented to verify that the model is predicting the trends correctly. During ATWS simulations, the available margin to any expected fuel damage amounts to several hundreds of degrees. This margin is more than adequate to account for uncertainties in the ability of TASC to predict PCT. This provides reasonable assurance that TASC can be used for ATWS predictions.

3.0 CONCLUSION

The staff has reviewed the TASC code as it is applied to LOCA, AOO, and ATWS analyses. The staff reviewed the physical models and their performance relative to experimental data. The staff concludes that there is reasonable assurance that TASC can be used in LOCA, AOO, and ATWS licensing calculations.

4.0 REFERENCES

1. NEDC-32084P, "TASC-03A, A Computer Program for Transient Analysis of a Single Fuel Channel," Rev. 2, October 2000.

2. A.C. Thadani (NRC) to J.S. Charnley (GE), "Team Audit of GE11 Fuel Design Compliance with Amendment 22 of NEDE-24011-P-A," March 24, 1992.

3. NEDO-20566-P-A, "General Electric Company Analytical Model for Loss-of-Coolant Analysis in Accordance with 10 CFR 50, Appendix K," September 1986.

Principal Contributor: A. Ulses

Date: March 13, 2002

Document Title: TASC-03A - A Computer Program for the Transient Analysis of a Single Channel

September 2002

ABSTRACT

The *TASC* code analyzes one-dimensional single channel hydraulic and heat transfer transients and calculates the local hydraulic conditions for a single channel and the rod temperatures for each rod group in that channel. It is used to calculate the change in critical power ratio during transient conditions.

A predictor-corrector scheme is employed for the solution of the two-phase transient thermal hydraulic equations. The drift flux formulation employed is particularly useful in handling problems typical of the loss-of-coolant accident analysis. The equations are valid for co-current upward or downward flow and counter-current flow. The treatment of counter-current flow limiting (CCFL) at restrictions, and the formation of two-phase levels is included. *TASC* can be run by specifying the bundle inlet flow or by specifying the pressure drop across the bundle.

Heat addition to the fluid is computed from a one-dimensional radial heat conduction model solved using the Crank-Nicholson method. The rods can be grouped together by local peaking factors, and separate temperature transients can be calculated for the various rod groups. Gamma-smeared heat generation is included. Both nuclear fuel rods and electrical heaters used in tests have been simulated by *TASC*.

Prepared by:

R. Harrington 6/17/2002
Engineer – Technology Development

Reviewed by:

R. W. Schrum 6/18/2002
Engineer – Nuclear Safety Analysis

Approved by:

G. A. Watford 7/03/2002
Manager – Fuel Engineering Services

Approved by:

J. F. Klapproth 7/08/2002
Manager – Engineering and Technology

Revision Status

Revision Number	Page	Description of Change	Signature
2	7, 39	*1.1 Addition of Lahey Mechanistic Subcooled Boiling Energy Distribution Model to Sections 2.1.1.1 and 3.6.2*	R. Harrington 6/16/00
	30	*1.2 Equation 3-6. "p_f" change to "ρ_f".*	
	35	*1.3 Equation 3-26. "V_f" and V_{fg}" changed to "v_f" and "v_{fg}"*	
	67	*1.4 Section 7 References. Addition of R.T. Lahey Reference.*	
	69	*1.5 Appendix A. "No" changed to "Yes" for SCAT Applicability to Fast Transients.*	
	69	*Appendix A. Addition of "Lahey Mechanistic" to TASC Subcooled Boiling Energy Distribution Models.*	
	77	*Appendix C. Equation Corrected to show* $\overline{T}_{cin} = \sigma T'_{cin} + (1-\sigma)T_{cin}$ *(T'_{cin} was missing " ' ".)*	

Table of Contents

Illustrations

Tables

1.0 INTRODUCTION

Transients in the nuclear power plant are analyzed using computer codes which have been verified against test data. The BWR transients are analyzed to obtain the limiting change in critical power ratio (ΔCPR) and the peak cladding temperature (PCT) as a function of time following the event, and the time of boiling transition. The ΔCPR is combined with the safety limit minimum critical power ratio (MCPR) to establish the operating limit MCPR. The models used for analyzing the transients are shown in Figure 1-1 and are employed to establish appropriate safety analysis limits as well as to analyze the reactor core response to all potential operating transients.

The subject of this report is that portion of the overall transient analysis process shown as Transient Critical Power (*TASC*) in Figure 1-1. *TASC* is a one-dimensional model which analyzes the most limiting bundles in the reactor core to determine the most limiting critical power ratio. The model was developed with sufficient flexibility to analyze a wide range of transient conditions. The types of transients that are analyzed are the same transients as analyzed by the One Dimensional Transient Analysis Model, *ODYN*, as described in Reference 1 [1]. Many of the transients take place in a matter of seconds. *TASC* can be used in the analysis of slower transients, those transients that take several minutes to complete, as well as the faster transients. Time Varying Axial Power Shapes (TVAPS) are used in the analysis of pressurization events. TVAPS is significant for ΔCPR evaluation during pressurization transients which result in reactivity insertion due to void collapse.

TASC is also used to calculate the early transient response of the limiting fuel bundle following a abnormal BWR operational transients such as the Loss of Coolant Accident (LOCA) and Anticipated Transients Without Scram (ATWS). Specifically *TASC* is used to calculate the early boiling transition for the fuel bundle for a LOCA and is used to calculated the peak fuel and cladding temperatures for the fuel bundle for ATWS. For the early LOCA analysis the system response is calculated by the blow down code *LAMB* [2]. The standard procedure for evaluating these events does not use TVAPS, but instead uses a constant axial power shape. This provides a conservative evaluation of the hot channel early boiling transition response during the first few seconds of a LOCA and provides a correct calculation of the decay heat distribution. For ATWS analysis the core transient boundary conditions are calculated by ODYN.

The *TASC* models are similar to the *SCAT* [2] models. The major differences are improvement to the numerical techniques and improved flexibility in the simulation of the bundle geometry allowing simulation of variable flow area and partial length fuel rods. Appendix A shows a comparison of the models used in the two codes. *TASC* was initially approved as a substitute for *SCAT* in the late 1980's [3]. *TASC* is an NRC approved methodology as documented in GESTAR II [4] and this *TASC* report serves to document the model.

TASC is a one-dimensional model which analyzes a single fuel bundle and is applicable for all fuel types. *TASC* predicts the thermal-hydraulic response to the BWR transient: the transient critical power ratio, the bundle fuel rod temperatures, the void fractions, the bundle pressure drop, and the initial onset of loss of nucleate boiling. The method for analyzing such transients employs

numerical treatment of the conservation equations. The approach is to write the conservation equation in Eulerian form which lends itself to donor-cell techniques. When sonic propagation effects are not important, the momentum equation can be decoupled from the continuity and energy equations. The continuity and energy equations are solved using a predictor-corrector method, and finally the momentum equation is integrated separately.

TASC receives transient information generated by the system codes such as *ODYN* or *LAMB*. The input information required by *TASC* is:

1. Bundle geometry.
2. Inlet flow versus time.
3. Inlet enthalpy of the reactor coolant versus time.
4. Bundle outlet pressure versus time.
5. The bundle axial and radial power distributions, as well as the total bundle power.

Four basic calculational models are used: (1) a Hydraulics Model used to determine the fluid flow through the channel. This model considers the state of the fluid at various levels within the channel – subcooled, nucleate boiling, and film boiling; (2) a Rod Conduction Model which considers the heat generation in the nuclear fuel rod; (3) a Heat Transfer Model that determines the heat transfer from the fuel rod to the fluid, both liquid and vapor, a determination based on the state of the fluid; (4) the Thermal Limits Model to determine the state of the fluid. Correlations for bubble departure enthalpy and energy distribution, pressure losses, subcooled boiling, etc. are used in the models. Figure 3-1 provides an overview of *TASC*, its models, and correlations and how they interact with one another.

The Hydraulics Model consists of a five-equation drift flux model – two mass and energy equations and a momentum equation. Section 2.1 provides the equations and the details of the Hydraulics Model. The Rod Conduction Model along with the bundle power calculational methodology is provided in Sections 2.2 and 2.3. The Heat Transfer Model is presented in Section 2.4; the Thermal Limits Model is presented in Section 3.1; and the correlations are described in the remaining Subsections of Section 3. Section 4 provides the qualification basis for *TASC*.

1.1 Overall Approach

During normal reactor operation subcooled water enters the fuel bundle from the lower plenum and experiences heating from the fuel rods. There are three different types of boiling heat transfer to water in forced convection systems: nucleate boiling, which is an extremely efficient mode of heat transfer, allowing large quantities of heat to be transferred with a very small temperature rise at the heated wall. As heat transfer rate is increased the boiling transfer surface alternates between film and nucleate boiling, leading to fluctuations in heated wall temperatures. The point of departure from the nucleate boiling region into the transition boiling region is called the boiling transition. Transition boiling begins at the critical power, and is characterized by fluctuations in cladding surface temperature. Stable film boiling occurs at the highest heat transfer rates; it begins as

transition boiling comes to an end. Film boiling heat transfer is characterized by wall temperatures which are significantly higher than those experienced during nucleate boiling.

TASC was developed to perform an assessment of the local hydraulic parameters (i.e., quality of the water and steam, void fraction, flow) over the range of anticipated transients. *TASC* is capable of performing hydraulic and heat transfer calculations in the single-phase liquid, two-phase nucleate boiling, two-phase film boiling, and single-phase vapor regimes. In the subcooled and in the film boiling regions, non-equilibrium phase temperatures are calculated. In the two-phase regime, cocurrent upflow and counter-current flow are modeled. Calculations of counter-current flow limiting (CCFL) and two-phase level movement can also be performed.

To handle the transient changes in power generation, a one-dimensional radial heat conduction model of the fuel rods is incorporated which generates the heat flux boundary condition associated with the energy equation. This also enables the code to track fuel rod temperatures during transients. The conduction model can be applied to several different types of rods grouped by local peaking and rod location.

In addition, power redistribution due to gamma smearing and direct moderating heating is calculated.

2.0 TECHNICAL DESCRIPTION

This section presents the governing conservation equations related to single-phase and two-phase transient hydraulics, and the heat conduction problem for the heat flux boundary condition to the hydraulics.

2.1 Thermal Hydraulics

The calculation of accurate thermal limits and heat transfer coefficients in a BWR fuel bundle is based upon the ability to predict the local thermal-hydraulic fluid conditions accurately. The thermal-hydraulic models used are designed to be flexible enough to handle a wide range of flow regimes and transients involving changes in pressure, flow, and power.

The numerical solution of the one-dimensional transient two-phase flow equations presented in the subsequent sections has the capability to model the effects of thermodynamic non-equilibrium, and rod-to-rod variation of heat flux. The numerics are designed to be capable of handling cocurrent upflow, countercurrent flow and cocurrent downflow. The numerical scheme utilized by the hydraulics package can be described as a predictor-corrector iterative scheme which allows for a semi-implicit solution of the governing equations.

The geometry of each axial node within the bundle is uniquely specified in terms of flow area, hydraulic diameter, and fuel rod heat transfer area. The axially variable geometry within the assembly allows the simulation of geometry changes that occur at the top of partial-length fuel rods. The specification of the nodal geometry variation due to partial-length fuel rods can be calculated given the number of partial-length rods and the heated and unheated length of these rods.

2.1.1 Governing Equations

Governing equations for subcooled boiling, nucleate boiling and film boiling are presented below. (Details of the derivation can be found in Appendix B.)

2.1.2 Boundary Conditions

The boundary conditions associated with the above equations are time dependent and can be specified in terms of bundle inlet flow or the imposed total pressure drop. For the inlet flow driven case, the boundary conditions consist of:

$W_\ell(0,t)$	=	Bundle inlet liquid flow rate (lbm/hr)
$W_g(0,t)$	=	Bundle inlet vapor flow rate (lbm/hr)
$P(t)$	=	System reference pressure (psia)
$q''(z,t)$	=	Bundle axial heat flux profile (Btu/hr/ft^2). The heat flux profile is obtained from a solution of the conduction heat transfer at each node interface within each rod group.
$h(0,t)$	=	Bundle inlet mixture enthalpy (Btu/lbm).

For a pressure drop driven case, the boundary conditions are:

$\Delta P(t)$	=	Bundle total pressure drop (psid)
$W_g(0,t)$	=	Bundle inlet vapor flow rate (lbm/hr)
$P(t)$	=	System reference pressure (psia)
$q''(z,t)$	=	Bundle axial heat flux profile (Btu/hr/ft^2). The heat flux profile is obtained from a solution of the conduction heat transfer at each node interface within each rod group.
$h(0,t)$	=	Bundle inlet mixture enthalpy (Btu/lbm).

If the liquid and vapor inlet flows are both zero ($W_\ell = W_g = 0$), the void fraction, α, is set to zero at the inlet and the inlet enthalpy is not used.

If $W_g \neq 0$ and $W_\ell \neq 0$ at the bundle inlet, the void fraction is calculated from an appropriate void correlation discussed in Section 3. If the bundle inlet is in counter current flow, the liquid flow is set to the minimum of the given flow and the CCFL limit. When the bundle inlet is single phase ($W_g \neq 0$, $W_\ell = 0$ or $W_\ell \neq 0$, $W_g = 0$), the fluid enthalpy is used along with the appropriate flow rate.

2.1.6 Leakage Flows

TASC has the capability of calculating leakage flows from the bundle to the surrounding bypass region for both flow driven and pressure drop driven options. The leakage path modeling considers flow from the bundle through the channel to lower tieplate casting gap, the gap between the lower tieplate and fuel support casting, and through the lower tieplate holes.

The hydraulic resistances of the fuel support orifice and lower tieplate must be specified (in terms of K/A^2) as well as the functional form of each leakage path flow in terms of the driving pressure difference. Each flow path is described and shown schematically in Figure 2-3. The functional form of the leakage flows is consistent with *ISCOR* [9].

2.1.7 Pressure Drop Driven Model

The pressure drop driver in *TASC* incorporates successive iterations on the total inlet flow until the input pressure drop is matched.

Figure 2-3. Leakage Flows

2.2 Radial Heat Conduction

Both BWR fuel rods and electrical heater test rod geometries are modeled and the rods can be arranged by user input into a maximum of five rod groups. *TASC* performs separate heat conduction and thermal limit calculations on each rod group. The surface heat flux is calculated using a one-dimensional radial heat conduction model.

The governing heat equation is fully discussed in Appendix C with the model developed to simulate a two-region fuel rod shown in Figure 2-4. The resulting heat conduction equation is

$$\rho C_P \frac{\partial T}{\partial t} = \frac{1}{r}\frac{\partial}{\partial r}\left(rk\frac{\partial T}{\partial r}\right) + \dot{q}''' \tag{2-35}$$

and the boundary conditions are given by

$$\begin{aligned}
-k\left.\frac{\partial \mathrm{T}}{\partial r}\right|_{r=r_n} &= q''(r_n,t) = H_\infty\left[\mathrm{T}(r_n,t) - \mathrm{T}_\infty(t)\right] \\
-k\left.\frac{\partial \mathrm{T}}{\partial r}\right|_{r=r_m} &= q''(r_m,t) = H_g\left[\mathrm{T}(r_{m-1},t) - \mathrm{T}(r_m,t)\right] \\
-k\left.\frac{\partial \mathrm{T}}{\partial r}\right|_{r=r_{m-1}} &= q''(r_{m-1},t) = \left(\frac{r_m}{r_{m-1}}\right) q''(r_m,t) \\
\left.\frac{\partial \mathrm{T}}{\partial r}\right|_{r=0} &= 0
\end{aligned} \tag{2-36}$$

where grid point n is at the outside surface of the cladding, point m is at the inside surface of the cladding, and point m – 1 defines the outside of the fuel rod region or the outside of the skin heater insulation material.

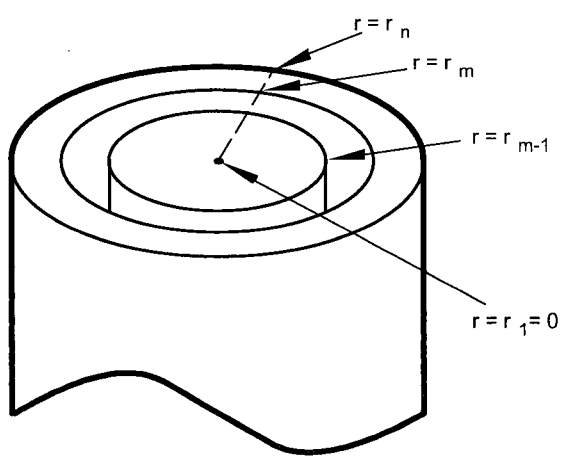

Figure 2-4. Typical Fuel Rod or Skin Heater

2.2.1 Electrical Heater Rod Geometry

In the comparison to test data, the performance of electrical heaters must be simulated. Described below is the *TASC* process for analyzing electrical heater performance.

As discussed by Equation 2-35, the solution to the one-dimensional heat conduction equation yields the temperature profiles at a given radius distribution. The radial noding used is an equal radius pattern and is different for fuel rods and heaters. For fuel rods, the radius distribution at every axial conduction elevation is the same.

2.3 Bundle Power Calculation

The *TASC* code contains four options for the calculation of the power in the bundle. First, the actual power in the bundle can be input. Second, the peak-linear heat generation rate (PLHGR) can be input and the bundle power can then be calculated. Third, the desired steady-state CPR can be input and the code iterates to obtain the bundle power. Fourth, all of the power can be put directly into the fluid, bypassing the conduction heat transfer model.

2.3.1 Gamma Energy Distribution

When simulating a BWR bundle in a thermal-hydraulic transient, the origin of the power is not as significant as the deposition of the energy in the surrounding rods and bundle hardware. It is the local deposition of energy which causes the fuel rods and cladding to heat up. The principal method of energy transfer from one location to another is through gamma ray and neutron transport.

2.5 Time Step Calculation

The time step logic incorporated into *TASC* tries to choose the largest time step which gives both stable and accurate results. Both the hydraulics and heat conduction models will supply recommended values for the time step. These values are then adjusted to give an optimum value.

2.5.1 Hydraulic Time Step

The recommended hydraulic time step is the minimum value based upon fluid transport time, level movement, and vaporization of the nodal liquid mass, time variation in void fraction, and the number of iterations it took to converge in the last time step.

2.5.2 Heat Conduction Time Step

The convergence of the solution is determined by estimating the second order term of the diffusion equation. That is,

$$E = \frac{\Delta t^2}{2} \frac{\partial^2 T}{\partial t^2} \tag{2-66}$$

TASC uses this expression to determine a relative error in the temperature calculation. The time step is limited such that the relative error is less than 0.001.

3.0 PHYSICAL CORRELATIONS

This section discusses the physical correlations used in *TASC*. The correlations include thermal limits, heat transfer, and drift flux relationships used to couple together the conservation equations discussed in Section 2, and the correlations used in making the pressure drop calculations. The flow chart in Figure 3-1 shows the coupling of the thermal hydraulics and heat conduction through the correlations, and details of the heat transfer and thermal limits correlations are summarized in Table 3-1.

3.1 Thermal Limits

Thermal limits calculations are performed in *TASC* for cocurrent flow boiling transition, and counter-current flow boiling transition. This is discussed in Subsection 3.1.1.

In co-current flow the *GEXL* [11] critical quality versus boiling length correlation is used.

The critical power ratio is one of the most important parameters calculated during the hydrodynamic solution since it determines when boiling transition occurs.

Figure 3-1. Correlation Coupling

Figure 3-2. Counter-Current Flow Dimensionless Critical Heat Flux

3.3 Drift Flux Parameters and Void Fraction Model

Void fraction correlation in *TASC* is of the "drift-flux" form originally proposed by Zuber and Findlay.

$$\alpha = \frac{j_g}{C_o j + \overline{V_{gj}}}$$

The distribution parameter and the drift velocity are provided by the Findlay-Dix Void Fraction correlation [16].

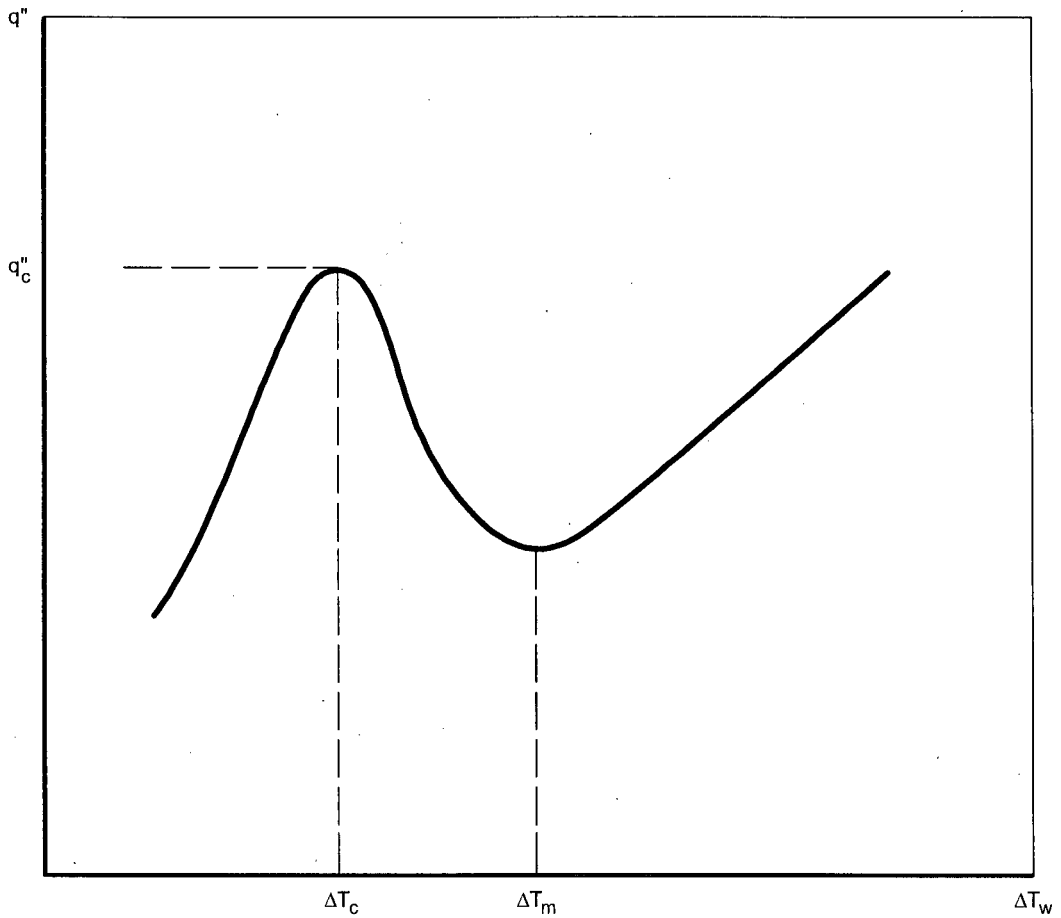

Figure 3-4. Transition Boiling Curve

4.0 QUALIFICATION STUDIES

To qualify *TASC*, results from the code were compared to measured transient test data taken at GE's ATLAS test facility and Blowdown Heat Transfer data (BDHT) taken at GE's Two Loop Test Apparatus (TLTA). A description of the input preparation for one transient case is discussed below with the knowledge that all the rest of the transient and BDHT cases are similar.

ATLAS test assemblies 28D, 32B, 35C, 56F, and 65D were used in the *TASC* qualification. The specific runs are described in Table 4-1. Typical pressure, power, and flow transient data for each assembly is shown in Figures 4-1 through 4-12. BDHT tests were also used in the TASC qualification as shown in Table 4-1. The BDHT tests were made to simulate loss of coolant accidents (LOCA) and are good examples of strong flow and power transients.

ATLAS transient test data was compared against *TASC* runs for GE9, GE11, GE12, GE13, and GE14 fuel design qualification. The specific runs are described in Table 4-2. Pressure, initial power, and flow transient data, which are representative of typical ATLAS test data for GE9 - GE14 fuel designs, for a Turbine Trip Transient with No Bypass (TTNBP) simulation are shown in Figures 4-13 through 4-15. Pressure, initial power, and flow transient data for an All Pump Trip Transient, which was simulated during the GE14 ATLAS tests, are shown in Figures 4-16 through 4-18.

In the ATLAS test facility the change in critical power ratio (ΔCPR) during a transient is determined by running a set of transients from the same initial conditions (pressure, subcooling and flow). Each test uses the same relative power, flow and pressure response (See Figures 4-13 to 4-17) and the initial power is gradually increased until a boiling transition is observed (a temperature increase of 50°C above saturation is used to indicate boiling transition). The initial critical power ratio (ICPR) is defined as the ratio of the critical power, Q_{ss}, at the initial conditions (pressure, subcooling and flow) to the initial power for the transient test, Q_t. Since the minimum critical power ratio at the onset of boiling transition is unity, the ratio of the change in initial critical power ratio to the initial critical power ratio is calculated as:

$$\frac{\Delta CPR}{ICPR} = \frac{ICPR - 1}{ICPR} = \frac{Q_{ss}/Q_t - 1}{Q_{ss}/Q_t} = \frac{Q_{ss} - Q_t}{Q_{ss}}$$

4.1 Input Preparation for ATLAS Cases

The procedure and input required to model the ATLAS bundle are illustrated in this section for assembly 56F, a full scale 64 rod bundle. The ATLAS 56F test series simulate turbine trip without bypass transients for a BWR/2-5 8x8 fuel bundle with and without a recirculation pump trip.

The input is separated into power, geometry, and transient inputs. The transient input is straightforward coming directly from the test data and will not be discussed. The geometry input is prepared based on the bundle description shown in Table 4-3 and Figure 4-19. The input preparation for modeling a BDHT bundle and a GE9 through GE14 tests is similar and is contained in References 18-22.

Figure 4-1. Pressure Versus Time Curve for Typical ATLAS 28D Runs

Figure 4-2. Power Versus Time Curve for Typical ATLAS 28D Runs

Figure 4-3. Inlet Mass Flux Versus Time Curve for Typical ATLAS 28D Runs

Figure 4-4. Pressure Versus Time Curve for Typical ATLAS 32B Run 115

Figure 4-5. Power Versus Time Curve for Typical ATLAS 32B Run 115

Figure 4-6. Inlet Mass Flux Versus Time Curve for Typical ATLAS 32B Run 115

Figure 4-7. Pressure Versus Time Curve for Typical ATLAS 35C Run 56

Figure 4-8. Power Versus Time Curve for Typical ATLAS 35C Run 56

Figure 4-9. Inlet Mass Flux Versus Time Curve for Typical ATLAS 35C Run 56

Figure 4-10. Pressure Versus Time Curve for Typical ATLAS 56F Run 27

Figure 4-11. Power Versus Time Curve for Typical ATLAS 56F Run 27

Figure 4-12. Inlet Mass Flux Versus Time Curve for Typical ATLAS 56F Run 27

Figure 4-13. Initial Power Versus Time Curve for Typical ATLAS TTNBP Simulation

Figure 4-14. Pressure Versus Time Curve for Typical ATLAS TTNBP Simulation

Figure 4-15. Inlet Mass Flux Versus Time Curve for Typical ATLAS TTNBP Simulation

Figure 4-16. Initial Power Versus Time Curve for Typical ATLAS All Pump Trip Simulation

Figure 4-17. Pressure Versus Time Curve for Typical ATLAS All Pump Trip Simulation

Figure 4-18. Inlet Mass Flux Versus Time Curve for Typical ATLAS All Pump Trip Simulation

Figure 4-19. Axial Locations of Spacers, Pressure Taps and Tubing Thermocouples for BWR/2-5 Bundle Tests (ATA 56)

4.1.1 ATLAS Power Distributions

The power input to a bundle can be distributed axially in the bundle, locally across the bundle, and radially across the fuel pellets. In the ATLAS simulation, all the power is generated in the clad by resistance type heating which implies that there is no radial distribution of power.

The axial power distribution is generated by varying the clad thickness in the axial direction. The ATLAS 56F bundle was manufactured to simulate a cosine shape power distribution given by,

$$P_{axial} = 1.398 \cos (0.01819 (Z-L/2))$$

where:

Z = axial position (inches)
L = bundle heat length (inches)

Since *TASC* can model only 5 rod groups, the 64 rods in the ATLAS 56F bundle must be grouped in such a way as to give a good simulation of both the heat transfer and the energy storage effects. The grouping of the rods is chosen based upon the bundle local peaking distribution and the distribution of the R-factors across the bundle. The R-factor parameter accounts for the effects of the fuel rod power distributions and the fuel assembly local spacer and lattice critical power characteristics. Its formulation for a given fuel rod location depends on the power of that fuel rod, as well as the power of the surrounding fuel rods.

For the ATLAS 56F bundle, the 64 rods were distributed in 5 rod groups. Table 4-4 shows the resulting *TASC* 5 rod groups. Rod group 2 is the simulated water rods in the 56F bundle. The other *TASC* qualification cases and fuel design qualification cases are divided into groups in a similar manner and Table 4-5 shows the limiting GEXL R-factors for the fuel design qualifications.

4.2 Input Preparation for Blowdown Heat Transfer (BDHT) Cases

The input preparation for modeling a BDHT bundle is exactly the same as the ATLAS bundles discussed in Section 4.1. The test simulated by TASC are summarized in Table 4-1. The experimental data for the BDHT tests were taken at GE's Two Loop Test Apparatus (TLTA) facility.

Test 4906 run 14 is the fourth problem in the NRC Standard Problem Series. Test 4904 run 45 is a high powered 7x7 bundle test and both test 6005 run 6 and 6414 run 3 are high powered 8x8 bundle tests. Test 6005 run 6 had no ECCS flow and Test 6414 run 3 had very low ECCS flow.

To illustrate the input procedure, test 4906 run 14 was chosen. Most of the input is self explanatory, however, the input preparation for some of the values requires additional explanation as discussed below.

4.2.1 BDHT Power Distribution

The axial power distribution for Standard Problem 4 is given by:

$$P_{axial} = 1.385 \sin\left[\frac{\pi(Z + 11.653)}{L + (2 \times 11.653)}\right]$$

where:

Z = axial position (inches)
L = bundle heat length (inches)

4.3 Comparison of TASC With ATLAS and BDHT Data

The initial boiling transition time (BT) predicted by *TASC* was compared with the measured ATLAS data and the measured BDHT data. The comparison data is shown in Table 4-6 and Table 4-7. A summary of the comparison is shown in Figure 4-20. Representative comparisons of clad temperature for BDHT are shown in Figures 4-22 through 4-25.

The ΔCPR/ICPR comparison of measured versus predicted results is summarized in Figures 4-21. The "GE12I" and "GE12Z" in the figure legend indicates an Inconel or Zircoloy GE12 spacer design. The data for this plot is shown in Table 4-8. Note that this table applies to cases at the

threshold of boiling transition (as opposed to Table 4-7 showing cases which have passed into boiling transition). When the fuel transcends into boiling transition the critical power ratio calculation is no longer applicable.

Figure 4-20. Time to Boiling Transition Comparison

Figure 4-21. Summary of Transient ΔCPR/ICPR Comparison

Figure 4-22. BDHT Test 4904 Run 45 Comparison of High Power Rod Peak Cladding Temperature

Figure 4-23. BDHT Test 4904 Run 45, 118 Inch Elevation Temperature Comparison

Figure 4-24. Test 4906 Run 14 Hot Rod Temperature 98 Inch Elevation Comparison

Figure 4-25. Test 4906 Run 14 Cold Rod Temperature 98 Inch Elevation Comparison

4.4 Conclusions

The verification runs have been performed with both skin heater and BWR geometries and operating conditions. The steady state solution of *TASC* for a BWR has been verified against that of the code *ISCOR* [9]. Comparisons of axial void and quality distribution, initial CPR, pressure drop, and leakage flow have been performed.

5.0 SENSITIVITY STUDIES

Two separate sensitivity studies were performed by varying the number of nodes and the timestep size to determine the effect on the Minimum Critical Power Ratio (MCPR) calculation. The MCPR can only be resolved within the ±0.01 uncertainty of the GEXL correlation and therefore differences less than ±0.005 are considered negligible. A GE11 turbine trip with no bypass and no recirculation pump trip transient having a cosine peaked power shape was used as input to *TASC* for these sensitivity studies.

5.3 Conclusions

TASC MCPR is not overly sensitive to a change in the number of heated hydraulic nodes or the timestep size. Studies show that even with large variations in the number of nodes and timestep size the resulting changes in MCPR are negligible.

6.0 NOMENCLATURE

A or A_F	–	Flow area (ft^2)
C_k	–	Kinematic wave velocity (ft/hr)
C_o	–	Void concentration parameter ( )
C_p	–	Specific heat of heater material (Btu/lbm-°F)
D_H	–	Hydraulic diameter (ft)
f	–	Single-phase fluid friction factor ( )
G	–	Mass flux (lbm/hr- ft^2)
g	–	Acceleration due to gravity (32.2 ft/sec^2)
g_c	–	Gravitational constant (32.2 lbm ft/lb_f sec^2)
H	–	Heat transfer coefficient from wall to fluid (Btu/hr-ft^2-°F)
H_g	–	Gap conductance (Btu/hr-ft^2-°F)
H_L	–	Heated length (ft)
H_o	–	Correlation constant for condensation (1/hr-°F)
h	–	Enthalpy (Btu/lbm)
J	–	Mechanical equivalent of heat, 778 (ft-lb_f/Btu)
j	–	Volumetric flux (ft/hr)
K	–	Irreversible loss coefficient associated with local flow obstructions ( )
K_W	–	Channel power (Btu/hr)
K_1	–	Film boiling vapor generation rate correlation constant ( )
k	–	Material conductivity (Btu/hr-ft°F)
L	–	Length (ft)
M	–	Momentum flux (lbm/hr^2-ft)
P	–	Reference pressure (psia)
P_F	–	Friction perimeter (ft)
P_H	–	Heated perimeter (ft)
P_i	–	Heat transfer perimeter at the phase interface (ft)
$P_k(Z)$	–	Axial power shape ( )
P_L	–	Local peaking factor ( )
Pr	–	Prandtl number ( )
q''	–	Local heat flux (Btu/hr- ft^2)
$\dot{q}'''$	–	Volumetric heat generation rate (Btu/hr-ft^3)
Re	–	Reynolds number ( )
r	–	Fuel rod radius (ft)
T	–	Temperature (°F)
TM	–	Thermal margin
T_W	–	Wall temperature (°F)
t	–	Time (hr)
u	–	Phase velocity (ft/hr)

$\overline{V}_{gj}$	–	Average drift velocity (ft/hr)
v	–	Local phase specific volume (ft^3/lbm)
W	–	Flow Rate (lbm/hr)
x	–	Flow quality ( )
x_e	–	Equilibrium quality ( )
X	–	Static quality ( )
Z	–	Axial position (ft)
α	–	Void fraction ( )
Γ *or* Γ_g	–	Volumetric vapor generation rate (lbm/hr-ft^3)
γ	–	Ratio of saturated vapor to liquid densities (ρ_g/ρ_f)
Δh_s	–	Channel inlet subcooling (Btu/lbm)
ε	–	Surface roughness used in Moody friction factors (inches)
ν	–	Specific volume (ft^3/lbm)
ρ	–	Density (lbm/ ft^3)
$\overline{\rho}$	–	Mixture density (lbm/ ft^3)
σ	–	Surface tension (lb_f/ft)
$\phi^2_{\ell i}$	–	Two-phase friction multiplier ( )
ϕ^2_{local}	–	Two-phase local loss multiplier ( )
< >	–	Area averaged

Subscripts

b	–	Boiling condition
c	–	Critical condition
f	–	Saturated liquid
g	–	Saturated vapor
H	–	Heated
i	–	Interface, node or previous time step
i + 1	–	Current time step
K	–	Kth node
K + 1	–	Upper interface of the Kth node
L	–	Local condition
ℓ or l	–	Liquid phase
m	–	Fuel rod material
p	–	Estimated at present time step
r	–	rth rod group
v	–	Vapor phase
w	–	Rod wall condition
∞	–	Bulk fluid condition

7.0 REFERENCES

3. MFN 059-89, Attachment 1 of the letter from JS Charnley (GE) to MW Hodges (NRC), *Application of Approved Methods To A New GE Fuel Design*, August 7, 1989.

5. N. Zuber, F. W. Staub and G. Bijwaard, *A Program of Two-Phase Flow Investigation, Eleventh Quarterly Report*, GEAP-5157, April 1966.

6. R. T. Lahey, *Two Phase Flow in Boiling Water Reactors*, July 1974, NEDO-13388.

7. P. Zaha and N. Zuber, "Point of Net Vapor Generation and Vapor Void Fraction in Subcooled Boiling," Proceedings of the 5th International Heat and Mass Transfer Conference, Toyko, 1974.

8. P. Saha, *A Post-Dryout Heat Transfer Model Based on Actual Vapor Generation Rate in Dispersed Droplet Regime*, NEDE-13443, May 1976.

11. *General Electric BWR Thermal Analysis Basis (GETAB): Data, Correlation and Design Basis*, NEDE-10958A, January 1977.

12. F. W. Dittus and L. M. K. Boelter, University of California (Berkeley), *Pub. Eng.*, Vol. 2, p. 443, 1930.

13. W. H. Jens and P. A. Lottes, *Analysis of Heat Transfer Burnout, Pressure Drop and Density Data for High Pressure Water*, USAEC Report ANL-4627, 1951.

14. R. S. Dougall and R. S. Rohsenow, *Film Boiling on the Inside on Vertical Tubes with Upward Flow of the Fluid at Low Qualities*, Massachusetts Institute of Technology, Department of Mechanical Engineering, Contract No. NSF G21455, Report No. 9079-26, September 1963.

15. J. E. Leonard, et at., *General Electric Company Analytical Model for Loss-of-Coolant Analysis in Accordance with 10CFR50 Appendix K – Amendment 1 – Calculation of Low Flow Film Boiling Heat Transfer for BWR LOCA Analysis*, NEDO-20566-1, January 1979, Revision 1.

17. J. Waggener, "Friction Factors for Pressure Drop Calculations," *Nucleonics*, Vol. 19 (No. 11), November 1961.

18. S. S. Kutateladze, "Elements of Hydrodynamics of Gas-Liquid Systems," *Fluid Mechanics –Soviet Research*, Vol. 1, No. 4, 29-50, 1972.

19. G. B. Wallis, *One-Dimensional Two-Phase Flow*, McGraw-Hill, New York, 1969.

20. O. C. Iloeje, et al., "An Inventory of the Collapse and Surface Rewet in Film Boiling in Forced Vertical Flow," Transaction of the ASME, May 1975.

Appendix A

APPENDIX B

Derivation of the One-Dimensional Transient Hydraulic Equations

APPENDIX C

Derivation of the One-Dimensional Radial Heat Conduction Conservation Equations

This Appendix describes the analytical model for transient radial conduction heat transfer (CHT).

C.1 Introduction

CHT solves the finite-difference equations obtained from the partial differential equations governing transient, radial conduction heat transfer in a solid or hollow cylinder. An arbitrary number of cylindrical regions can be specified (fuel and cladding, two fuel regions with different physical properties and cladding, etc.), and an arbitrary number of nodes (minimum of two) can be used in each region, when CHT is incorporated into other codes. The main program provided is limited to 5 regions or less and a total of 50 or fewer nodes for all regions. A typical geometry is shown in Figure C-1.

A gap can be specified between one or more regions, or regions can be used without a gap between them.

The properties are a function of temperature; the heat transfer coefficients and fluid temperature(s) are an input function of time, and the heat generation is a function of time and radial position. Different sets of properties can be input for each region. No axial variations are considered.

CHT is a variable implicit code (explicit, Crank-Nicholson, pure implicit or something intermediate can be used). The purely implicit method is recommended for use in TASC.

Any consistent set of units can be used in CHT.

C.2 Analysis

C.2.1 Explicit and Implicit Methods

Three basic finite-difference formulations can be considered, depending upon the time at which the spatial derivatives and physical properties are evaluated. If the derivative is evaluated at the previous time step, the method is an explicit one. If the derivative is evaluated at the new time step, the method is called a pure implicit, completely implicit, or fully implicit method. If the derivative is found by averaging values at the new and old time steps, a Crank-Nicholson equation results.

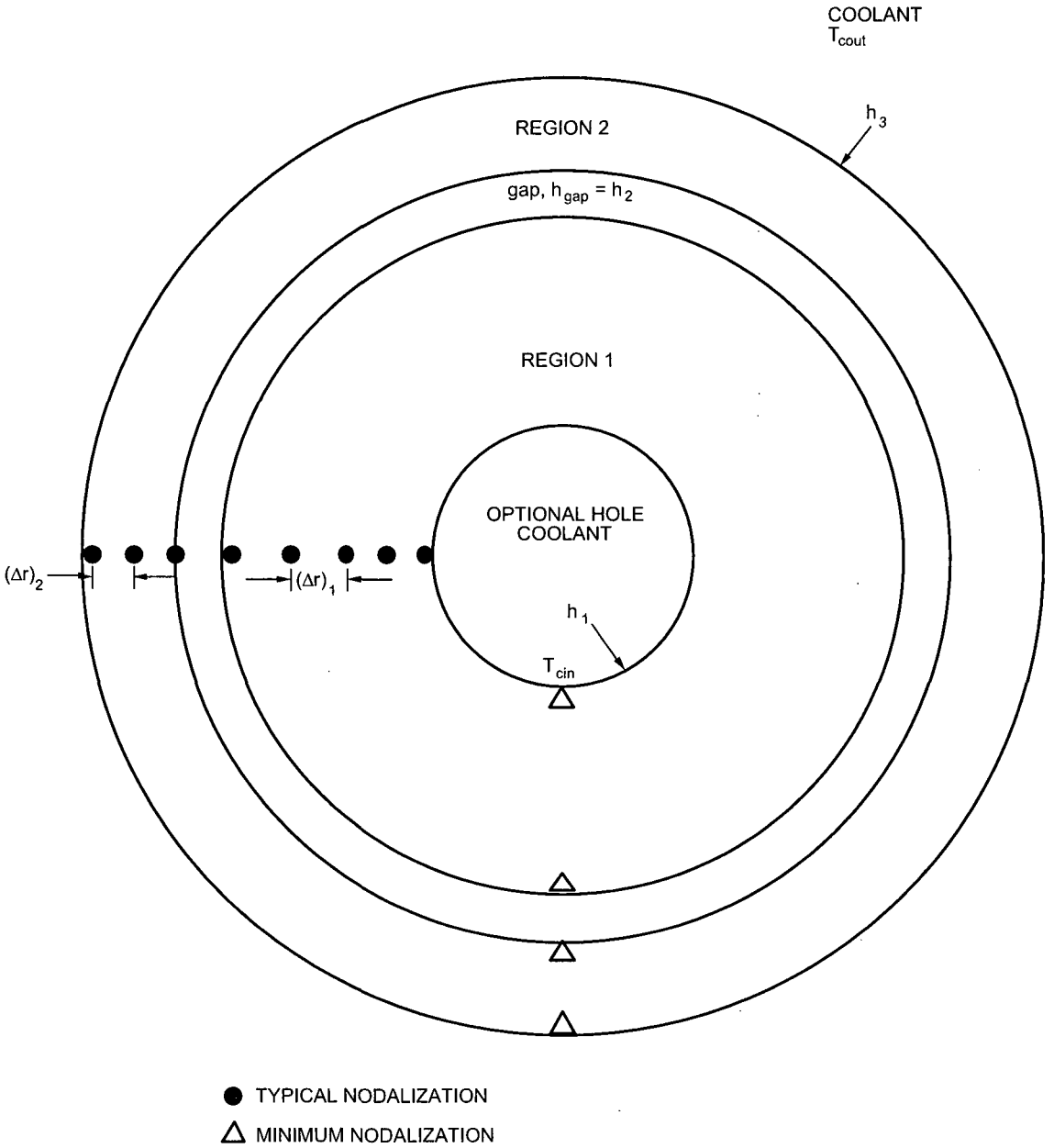

Figure C-1. Sample Geometry and Nodalization

The three methods are summarized by the following equation (nomenclature is defined in Section C.4):

$$\frac{\partial}{\partial r}\left(k\frac{\partial T}{\partial r}\right)=\frac{1}{(\Delta r)^2}\left[\frac{(k_{i-1}+k_i)}{2}\overline{T}_{i-1}-\frac{(k_{i-1}+2k_i+k_{i+1})}{2}\overline{T}_i+\frac{(k_i+k_{i+1})}{2}\overline{T}_{i+1}\right]$$

where r is the radial position, t is time, and $\overline{T} = \sigma T' + (1 - \sigma)T$, is a weighted average between the temperatures at the new and old times. Sigma, σ, has the following values for the three methods:

σ = 0, Explicit method

σ = 0.5, Crank-Nicholson method

σ = 1, Pure implicit method

The explicit method is unstable if the time increment, Δt, exceeds a critical value; the Crank-Nicholson method is stable for all time steps, but oscillations (stable) can occur for large time steps. The pure implicit method damps oscillations whose period is less than the timestep so timestep size determines the fidelity of the results.

C.2.2 Derivation of Finite-Difference Equations

The finite-difference equations can be obtained by considering an energy balance on representative nodes. The conservation of energy equation for this case is

rate of change in stored energy	=	rate of energy in	–	rate of energy out	+	rate of energy generation	(C-1)

In general, three-nodes are considered for each finite-difference equation. By definition, consider energy in to be heat transferred from the adjacent node closest to the center of the cylinder to the middle node of the three. Energy out is heat transferred from the middle node to the next node farther from the center.

C.2.2.1 The First Node of the First Region

Consider a hollow interior with convection to a liquid at $\overline{T}_{cin}$ where the bar indicates a weighted average between values at the old and new times,

$$\overline{T}_{cin} = \sigma T'_{cin} + (1-\sigma)\,T_{cin}$$

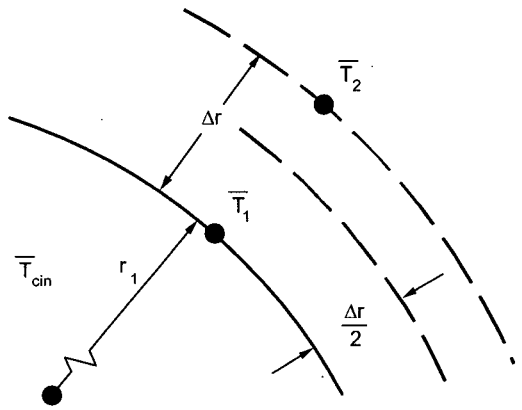

Change in stored energy $= \rho C_p V \dfrac{\partial T}{\partial t} = \dfrac{(\rho C_p V)_i}{\Delta t}(T_i' - T_i)$

Energy in $= h_1 A_1 (\overline{T}_{cin} - \overline{T}_1)$,

Energy out $= k_B A_m \dfrac{(\overline{T}_1 - \overline{T}_2)}{\Delta r}$

where k_B is the average of the thermal conductivities at nodes 1 and 2.

Energy generated $= \dot{Q}'''_1 V_1$,

A_1 is the interior surface area.

$A_1 = 2\pi r_1 \ell$ or $r_1 \ell$ per radian,

V_1 is the area of the volume element,

$$V_1 = \pi\ell\left[\left(r_1 + \frac{\Delta r}{2}\right)^2 - r_1^2\right] = \pi\ell\left(r_1 + \frac{\Delta r}{4}\right)\Delta r,$$

or

$$V_1 = \ell\left(r_1 + \frac{\Delta r}{4}\right)\frac{\Delta r 2}{2} \text{ per radian}$$

A_m is the mean heat transfer area; that is, the area halfway between nodes 1 and 2.

$$A_m = 2\pi\ell\left(r_1 + \frac{\Delta r}{2}\right) = \ell\left(r_1 + \frac{\Delta r}{2}\right) \text{ per radian.}$$

Combining the above equations gives the coefficients a_i, b_i, c_i and d_i for the first finite-difference equation,

$$a_i T'_{i+1} + b_i T'_i + c_i T'_{i+1} = d_i.$$

The coefficients are given in Table C-1.

For steady-state conditions, the coefficients can be found by multiplying d_i by $\rho C_p/\Delta t$ and letting $\rho C_p \rightarrow 0$. The resulting coefficients are given in Table C-2.

C.2.2.2 First Node for Solid Cylinders

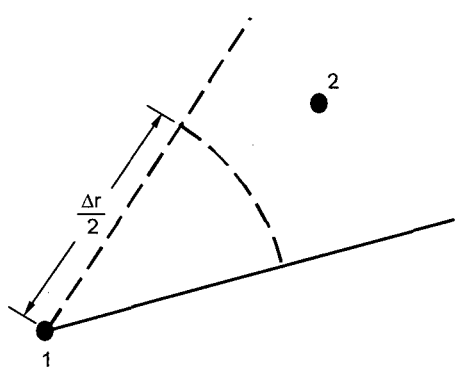

$$V_1 = \frac{\pi\ell\left(\frac{\Delta r}{2}\right)^2}{2\pi} = \frac{(\Delta r)^2}{8}\ell \text{ per radian.}$$

$$A_m = 2\pi\ell\frac{\Delta r}{2}\frac{1}{2\pi} = \frac{\ell\Delta r}{2} \text{ per radian.}$$

For this case, r_1 and h_1 are zero. There is no energy into node 1 due to symmetry. Otherwise, the derivation is similar to that given in Subsection C.2.2.1. The coefficients obtained are given in Table C-1.

C.2.2.3 Interior Nodes

For interior nodes, it is simpler to obtain the finite-difference equations from the partial differential equation than from an energy balance. The differential equation is

$$\rho C_p \frac{\partial T}{\partial t} = \frac{\partial}{\partial r}\left(k\frac{\partial T}{\partial r}\right) + \frac{k}{r}\frac{\partial T}{\partial r} + \dot{Q}'''$$

The stored energy term is approximated by

$$\frac{(\rho C_p)_i}{\Delta t}(T'_i - T_i)$$

The first conduction term, containing the thermal conductivity within the derivative, is given by

$$\frac{\partial}{\partial r}\left(k\frac{\partial T}{\partial r}\right) \approx \frac{1}{(\Delta r)^2}\left[\frac{(k_{i-1}+k_i)}{2}\overline{T}_{i-1} - \frac{(k_{i-1}+2k_i+k_{i+1})}{2}\overline{T}_i + \frac{(k_i+k_{i+1})}{2}\overline{T}_{i+1}\right],$$

where $\overline{T}$ is a weighted average between the temperatures at the new and old time:

$$\overline{T} = \sigma T' + (1-\sigma)\,T.$$

The first derivative term can be approximated by

$$\frac{k}{r}\frac{\partial T}{\partial r} \approx \frac{1}{2}\frac{1}{r_i}\left[\frac{(k_i+k_{i+1})}{2}\frac{(\overline{T}_{i+1}-\overline{T}_i)}{\Delta r} + \left(\frac{k_{i-1}+k_i}{2}\right)\frac{(\overline{T}_i-\overline{T}_{i+1})}{\Delta r}\right]$$

The coefficients, a_i , b_i, c_i, and d_i, are given in Table C-1.

C.2.2.4 Last Node of Annular Regions

The coefficients for the last node of an annular region depend upon whether or not the region is adjacent to the coolant. For the last node of any region, the geometry is shown in the following sketch:

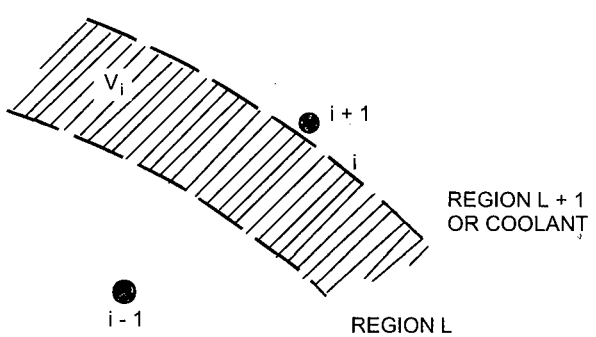

If region L is the last region ($L = L_{max}$), then $\overline{T}_{i+1}$ is the coolant temperature; and if region L is an interior region, $\overline{T}_{i+1}$ is the first node of the next region.

The volume of the last node of any region, per radian, is

$$v_i = \left[\pi r_i^2 - \pi\left(r_i - \frac{\Delta r}{2}\right)^2\right]\frac{\ell}{2\pi} = \left(r_i - \frac{\Delta r}{4}\right)\ell\frac{\Delta r}{2}.$$

The mean heat transfer area, per radian, is

$$A_m = \left(r_i - \frac{\Delta r}{2}\right)\ell,$$

and the surface area of the region, per radian, is

$$A_i = r_i\,\ell.$$

The energy into the volume element consists of the energy entering the shaded area by conduction, plus the energy generated. The conduction from i-1 to i is

$$\left(\frac{k_{i-1} + k_i}{2}\right)A_m\frac{\left(\overline{T}_{i-1} - \overline{T}_i\right)}{\Delta r}.$$

If the region is not the last region, the energy out is the energy transferred across the gap:

$$h_{L+1}\,A_i\left(\overline{T}_i - \overline{T}_{i+1}\right).$$

If the region is the last region, $\overline{T}_{i+1}$ is replaced by the coolant temperature, which is assumed to be a known quantity.

The stored energy term and the heat generation term are approximated as it was done for the other nodes. The coefficients, a_i, b_i, c_i, and d_i, are given in Table C-1.

When a physical gap exists between two regions, the gap heat transfer is accounted for by using a gap conductance. The heat transfer is based upon the outside surface area of the inner region of the two regions being considered.

C.2.3 Equations for an Interface Between Two Regions with no Gap

If any two regions exist without a gap between them ($h \rightarrow \infty$ theoretically), the coefficients are renumbered so only one of the "collapsed" boundary nodes at the same radial location is included in the tri-diagonal matrix. After the tri-diagonal matrix is solved (Section C.4), the nodes are again renumbered (back to the original numbering), setting the two identical nodes equal to the same value of temperature. If this were not done, the matrix would not be tri-diagonal and a more complicated solution method would be required. The equations for this case are discussed as follows.

In this case Equation C-1 is applied to the following sketch

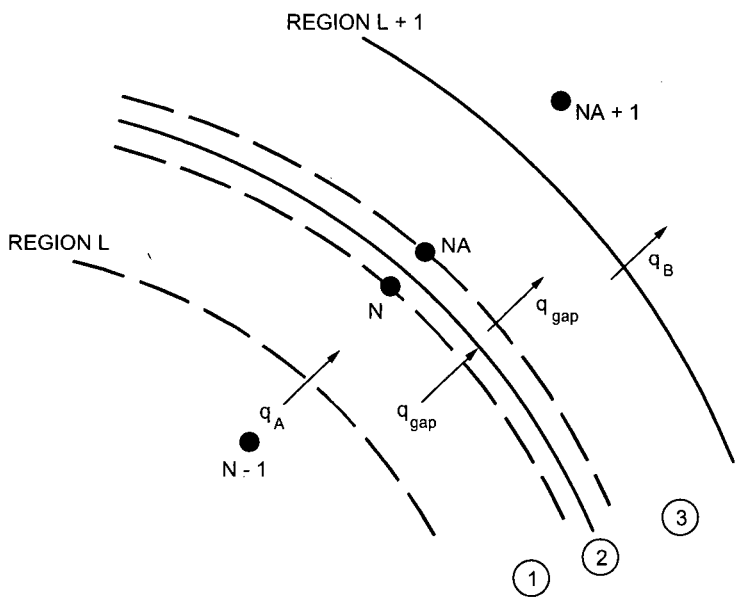

where

q_A is the conduction heat transfer entering control volume ①,

q_{gap} is the heat transfer leaving control volume ① and control volume ② and also the heat transfer entering control volumes ② and ③,

q_B is the heat transfer leaving control volume ③,

and N and NA are the two nodes that are collapsed into one node.

The conservation of energy equations for the three control volumes are

$$q_A - q_{gap} + \dot{Q}''' {}_N V_N = \left(\rho C_p V\right)_N \frac{\partial T_N}{\partial t} \qquad (C-2)$$

$$T_N = T_{NA} \qquad (C-3)$$

$$q_{gap} - q_B + \dot{Q}''' {}_{NA} V_{NA} = \left(\rho C_p V\right)_{NA} \frac{\partial T_N}{\partial t} \qquad (C-4)$$

where

V_{NA} is the volume of control volume ③,

Q'''_{NA} is the heat generation in control volume ③,

and the other symbols have their usual meaning (see Section C.3).

The finite-difference forms of Equations C.2.2 and C.2.4 are

$$\frac{-k_A A_A\left(\overline{T}_N - \overline{T}_{N-1}\right)}{\Delta r_L} - q_{gap} + \dot{Q}''_N V_N = \frac{\left(\rho C_p V\right)_N}{\Delta t}\left(T'_N - T_N\right)$$

(C-5)

$$q_{gap} + \frac{k_B A_B}{\Delta r_{L+1}}\left(\overline{T}_{NA+1} - \overline{T}_{NA}\right) + \dot{Q}''_{NA} V_{NA} = \frac{\left(\rho C_p V\right)_{NA}}{\Delta t}\left(T'_{NA} - T_{NA}\right) \qquad \text{(C-6)}$$

where

$$A_A = \left(r_N - \frac{\Delta r_L}{2}\right)\ell$$

$$A_B = \left(r_{NA} + \frac{\Delta r_{L+1}}{2}\right)\ell$$

$$V_N = \left(r_N - \frac{\Delta r_L}{4}\right)\frac{\ell\,\Delta r_L}{2}$$

and

$$V_{NA} = \left(r_{NA} + \frac{\Delta r_{L+1}}{4}\right)\left(\frac{\ell\,\Delta r_{L+1}}{2}\right)$$

Letting

$$\Psi = \Delta t/(\rho_N C_{PN} V_N + \rho_{NA} C_{PNA} V_{NA}),$$

$$\overline{T} = \sigma T' + (1 - \sigma)T$$

and combining Equations (C-3), (C-5) and (C-6) results in the coefficients for the finite-difference equation for the collapsed node. The coefficients are given in Table C-3.

C.3 Matrix Solution Method

The finite-difference equations obtained in the present case involve, in general, three unknown temperatures at the new time, t + Δt. The matrix of the coefficients is tri-diagonal and has the following form:

$$b_1 T'_1 + c_1 T'_2 = d_1$$

$$a_2 T'_1 + b_2 T'_2 + c_2 T'_3 = d_2$$

$$a_3 T'_2 + b_3 T'_3 + c_3 T'_3 = d_3$$

$$\vdots \qquad \vdots \qquad \vdots \qquad \vdots$$

$$a_{n-1} T'_{n-2} + b_{n-1} T'_{n-1} + c_{n-1} T'_n = d_{n-1}$$

$$a_n T'_n + b_n T'_n = d_n$$

This system of equations can be solved by recursion formulas. Let

$$c_1^* = \frac{c_1}{b_1}, d_1^* = \frac{d_1}{b_1},$$

$$c_{i+1}^* = \frac{c_{i+1}}{b_{i+1} - a_{i+1} c_i^*}; d_{i+1}^* = \frac{d_{i+1} - a_{i+1} d_i^*}{b_{i+1} - a_{i+1} c_i^*}$$

$i = 1, \ldots, n-1.$

Then

$$T'_n = d_n^*$$

$$T'_i = d_i^* - c_i^* T'_{i+1} \qquad i = n-1, n-2, \ldots, 1.$$

Table C-1
Transient Finite-Difference Coefficients

Table C-2
Steady-State Finite-Difference Coefficients

Table C-3

C.4 NOMENCLATURE

Any consistent set of units can be used in CHT.

a_i, b_i, c_i, d_i	Coefficients in finite-difference equations
C	Constant
Cp	Specific heat,
f(t)	Dimensionless decay heat, function of time
GAP (L – 1)	Radial distance between regions L – 1 and L
h_L	Heat transfer coefficient between a surface and the fluid, or between two regions
k	Thermal conductivity
k_A	[k(I–1) + k(I)]/2
k_B	[k(I) + k(I+1)]/2
m_2	$\rho Cp\ (\Delta r)^2/k_B\ \Delta t$
N	Number of nodes
P_f	Radial peaking factor in a region, a function of r
P_{ci}	Stability (accuracy) parameter defined in Table C-1.

q_l''', $\dot{Q}'''$	Heat generation, energy/(time • volume)
R(L)	Outer radius of region L-1
r	Radial coordinate
r_i	Radial location of the ith node
Δr	Distance between nodes. It can be different for each region.
t	Time
Δt	Time increment
T_i'	Temperature at new time ($t+\Delta t$) at node i
T_i	Temperature at old time (t) at node i
$\overline{T}$	$\sigma T' + (1 - \sigma)\, T$
T_{cin}	Fluid temperature inside cylinder
T_{cout}	Fluid temperature outside cylinder
V_i	Volume of ith node
$W1_i$	$[4(2\, r_i + \Delta r)/(4\, r_i + \Delta r)]/(\Delta r)^2$
$W2_i$	$[4(2\, r_i - \Delta r)/(4\, r_i - \Delta r)]/(\Delta r)^2$
$W3_i$	$[8\, r_i\, \Delta r/(4\, r_i + \Delta r)]/(\Delta r)^2$
$W4_i$	$[8\, r_i\, \Delta r/(4\, r_i - \Delta r)]/(\Delta r)^2$
$W5_i$	$[1 + \Delta r/(2\, r_i)]/(\Delta r)^2$
$W6_i$	$[1 - \Delta r/(2\, r_i)]/(\Delta r)^2$
ρ_L	Density in region L

	0,	explicit method
σ	0.5,	Crank-Nicholson method
	1,	pure implicit method

APPENDIX D

Void Fraction Model and Drift Flux Parameters